An Experimental Evaluation of the Gerdemann–Jablonski Compaction Equation

RONALD MACHAKA and HILDA K. CHIKWANDA

This paper reports on an attempt to independently evaluate the validity and applicability of a new compaction equation recently presented by Gerdemann and Jablonski [*Metallurgical and Materials Transactions A*, **42** (2011) 1325–1333] using experimental data. Furthermore, the rationality of Gerdemann and Jablonski's interpretation of the equation parameters is examined. The results are discussed in terms of the comparative evaluation of four different titanium powders (sponge Ti, CP TiH_2, Grade 2 CP Ti, and TiH_2-SS316L nanocomposite blend prepared by high energy milling) cold pressed in die to compaction pressures of up to 1300 MPa.

DOI: 10.1007/s11661-015-2793-8

I. INTRODUCTION

POWDER compaction equations are essentially mathematical descriptions of the compaction process. Paronen and Llkka[1] have compiled a comprehensive list of the powder compaction equations. Diversity in the formulation of the equations is clearly visible. The majority of the compaction equations attempt to empirically model the compactibility *vs* applied pressure profiles.

According to Bockstiegel,[2] the interest in powder compaction equations was initially motivated by a practical problem—the need to be able to predict the compaction pressures required to achieve a certain density. Today compaction equations find applications across materials science research themes (from powder metallurgy, nanostructured powders, pharmaceuticals, ceramics, soils, to even agricultural biomass materials) and across compaction routes (including cold, hot, and dynamic compaction), as reflected in the literature.[1–11]

Managing application approaches or deducing valid interpretations is some of the practical problem with complex equations. On the other hand, simplistic equations tend to yield poor or insufficient information. It is therefore not surprising that the interest in powder compaction equations has since shifted more toward an analytical problem—finding a 'simple but adequate' mathematical description for experimentally observed compaction curves.[2,12]

Recently, a persuasive criterion of an ideal compaction equation was put forth as "one whose parameters relate in some way to the basic physical and mechanical properties of the material being compacted".[12] Thus, 'simple but adequate' equations that only predict compaction density *vs* pressures profiles alone are worthless, especially if they cannot characterize the multi-stage compaction process and unearth underlying mechanisms driving densification.

Studies into the cold compaction of titanium and titanium-based powder materials are necessitated by the fact that titanium powder metallurgy offers a cost and energy-consumption reduction benefit—given the high cost of titanium powder material.[13] In addition, challenges associated with titanium powder compaction such as (i) an obvious high reactivity of titanium powder material in air, (ii) its inherent difficulty to press into green bodies due to its high hardness and inductile properties,[14] (iii) problems associated with compact cold welding to the die wall[14–18] as well as (iv) the high ejection force required,[14,16,17] for example, further justify the continued interests in the cold compaction behavior of titanium powders. However, although many researchers report on the compressibility behavior of titanium powders,[4,5,13,14,17,19–21] yet only a relative few apply the existing or new compaction models to the analysis of the cold compaction behavior of the powders.[15,22,23]

Gerdemann and Jablonski in Reference 4 recently proposed a new densification equation. They validated their proposed empirical model using eight titanium powder materials with different powder characteristics (powder chemistry and particle size and shape). Their results demonstrate that regardless of powder characteristics, the densification of titanium powders material can be modeled accurately, with respect to applied pressure, as the sum of the powder material's initial bulk density and the contributions of the powder particle rearrangement and work hardening (plastic and elastic) mechanism terms.

The Gerdemann and Jablonski equation, *in its published form*, is shown in Eq. [1] below:

$$D = D_0 + A\left(1 - e^{-bP}\right) + B\left(1 - e^{-bP}\right), \qquad [1]$$

where D_0 represents an initial density, parameters A and B reflect the relative contribution of powder rearrange-

RONALD MACHAKA, Senior Researcher, and HILDA K. CHIKWANDA, Research Group Leader, are with the Titanium Centre of Competence, Council for Scientific and Industrial Research, P.O. Box 395, Pretoria 0001, South Africa, and also with the Light Metals, Materials Science and Manufacturing, Council for Scientific and Industrial Research, Office F7, Building 14F, P.O. Box 395, Pretoria 0001, South Africa. Contact e-mail: RMachaka@csir.co.za
Manuscript submitted September 2, 2014.

Published online: 18 February 2015

ment and work hardening mechanisms to densification, respectively, and according to Gerdemann and Jablonski[4] parameters a and b reflect how much pressure is required to bring each mechanism to completion. The maximum density achievable by compaction alone, D_∞, is the sum of D_0, A, and B.

It is clearly by typographical error that the parameter, 'a', was defined and deduced by curve fitting when it is not used in Eq. [1].

The foremost focus of this technical paper is to independently evaluate the validity and applicability of the recently proposed empirical compaction.[4] Furthermore, the rationality of Gerdemann and Jablonski's interpretation of the 'a and b' model parameters is examined. The results of this study are discussed in terms of the compaction behavior of four different titanium powder materials investigated.

II. EXPERIMENTAL BACKGROUND

Four different titanium powder materials are investigated in this study; sponge Ti powders, TiH_2 powders, CP Grade 2 Ti powders, and TiH_2-SS316L nanocomposite powders. The 50 wt pct TiH_2 to 50 wt pct SS316L nanocomposite powder material was prepared by mechanically milling TiH_2 powder supplied by AG Materials Inc. (particle size 10 to 35 μm) and Type 316L stainless steel powder material supplied by Höganäs AB (particle size 20 to 53 μm).

The mechanically milling was conducted using Simoloyer CM01-21 instrument (Zoz GmbH) with a stainless steel vial sealed with a rubber 'O' ring and filled with argon gas to prevent contamination. A 20:1 ball-to-powder mass ratio, a rotation speed of 800 rpm, and 5-mm stainless steel balls were employed; no process control agent was used.

The particle size and shape analysis of the four starting powder materials were done using the Microtrac Bluewave laser particle analyzer (Microtrac Inc, Bluewave, USA) using distilled water as the dispersant. The morphology of all the starting powder materials was investigated by scanning electron microscopy (SEM) using the JEOL JSM-6510 scanning electron microscope (JEOL, Japan). Furthermore, X-ray diffraction analysis was carried out to determine the crystallite size of the milled TiH2 to S316L nanocomposite powder material on a PANalytical X'Pert PRO powder diffractometer (PANalytical, Netherlands).

The loose bulk density of each of the starting powder materials was determined using the graduated cylinder approach in accordance with the standard test method for determining loose and tapped bulk densities of powders (ASTM D7481-09), specifically Method A.[24] The initial porosity values indicated in Table I below are intended to give an indication of the relative void space in each of the studied starting powder material. The values are averages of five carefully taken measurements for each material. The initial porosity values were not measured directly; they were calculated from the bulk density and particle density using $\text{Porosity} = 1 - \frac{D_b}{D_p}$, where D_p represents the powder particle density, and D_b represents the loose density, see also Reference 25.

Each powder material was uniaxially pressed (double action compression) at different pressure levels up to 1250 MPa. A reinforced tool-steel split-die with a 13.81-mm inside diameter was used. Compacted samples with nominal aspect ratios (height to diameter) between 0.5, and 0.3 were obtained.

No internal lubrication was used. However, before each cycle, the die walls and punch surfaces were sparingly lubricated with zinc stearate spray. All powders were pressed at room temperature.

The as-pressed samples were weighed with a precision mass balance. The volume of the compacted samples was calculated from at least five diameter and height measurements with a Vernier calliper. From the mass and calculated volume, the samples' densities were deduced. The Archimedes' method density results were on average less than 1 pct higher; however, they were not used because of an inconsistency in the open pore sizes especially toward lower densities.

III. RESULTS AND DISCUSSION

A. *Powder Properties*

By observation, the size distributions and morphologies of the powder material particles are evidently widely varied. The particle size and shape analysis results are summarized in Table I. SEM images of the starting materials used for this study are shown in Figures 1(a) through (d).

Particle size analysis of the TiH_2-SS316L nanocomposite blend determined by laser diffraction shows that powder has a bimodal distribution with sizes between 1.51 μm (D_{10}) and 72.66 μm (D_{90}). The measured particle size distribution is in agreement with the observed SEM image presented in Figure 1(d). 24 pct by volume of the sampled material was determined to be the smaller particles with a mode radius of as 1.73 μm while 76 pct by volume was determined to be the larger particles with a mode radius of as 32.34 μm. However, the average crystallite size in the nanocomposite blended composite powders was determined to be 15 nm from the X-ray diffraction data using the Scherrer equation.

Particle shape analysis as determined by laser diffraction is also shown in Table I in terms of two different shape descriptors; average sphericity and average roundness. The particle morphology of the Sponge Ti and TiH_2 particles is irregular while that of Grade 2 Ti powders is spherical. However, the particle shapes in the TiH_2-SS316L nanocomposite powders are mixed with an average sub-rounded particle roughness and medium sphericity; the nanocomposite powder does have an average aspect ratio of 1.54.

B. *The Gerdemann–Jablonski Equation*

The omission of parameter 'a' in the published form of the Gerdemann–Jablonski equation is clearly a

Table I. Powder Characteristics of the Materials Under Examination in this Work

Material	Ti Sponge	TiH_2	CP Grade 2 Ti	MA TiH_2-SS316L
Supplier	Industrial Analytical (Pty) Ltd	AG Metals Inc.	TLS Technik GmbH & Co.	—
Particle characteristics				
Mean sphericity	0.844	0.825	0.887	0.845*
Mean roundness	0.683	0.671	0.804	0.633*
Size, D_{10} (μm)	159.4	11.4	22.8	*
Size, D_{50} (μm)	250.0	18.7	32.1	*
Size D_{90} (μm)	668.0	28.6	41.06	*
Morphology	spongy	angular	spherical	mixed*
Theoretical density (g/cm^3)	4.51	3.76	4.51	5.56
Initial porosity (pct)	82.3	62.3	45.4	62.6

*Symbol indicates a bimodal particle size distribution and character, see also Fig. 1(d).

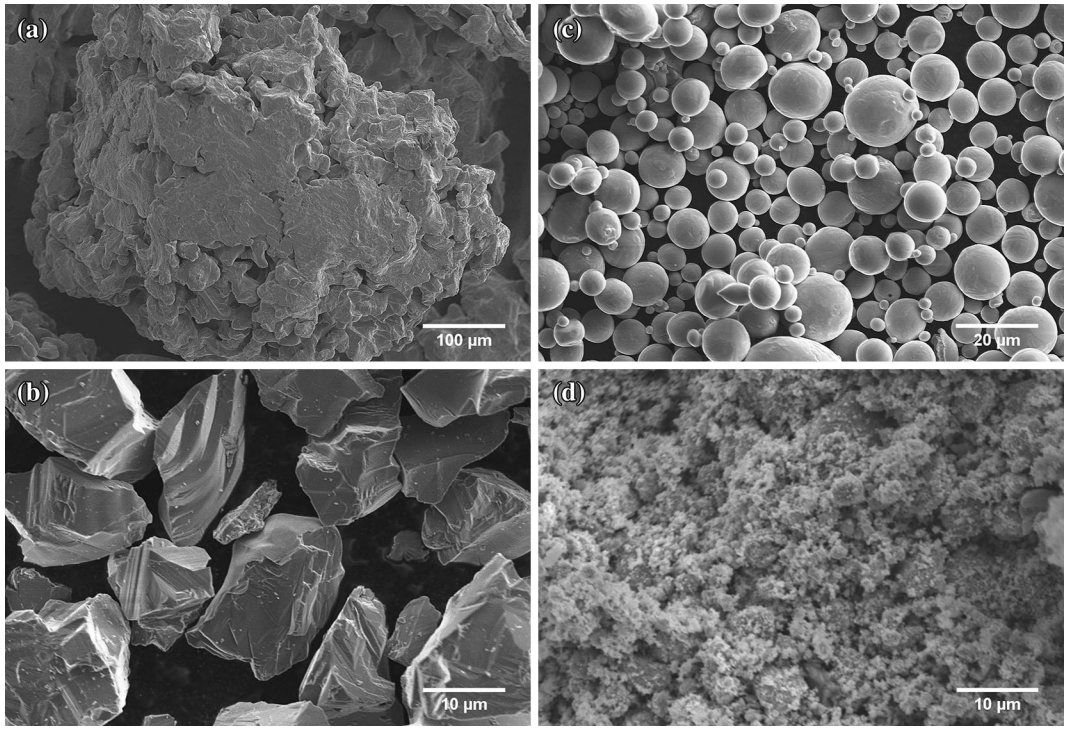

Fig. 1—SEM images of (*a*) sponge Ti powder, (*b*) TiH_2 powder, (*c*) CP Grade 2 Ti powder, and (*d*) TiH_2-SS316L-blended composite powders after 8 h of high energy mechanical milling, respectively.

typographical error—the corrected form of the published equation is shown in Eq. [2] below:

$$D = D_0 + A\left(1 - e^{-a\mathrm{P}}\right) + B\left(1 - e^{-b\mathrm{P}}\right) \qquad [2]$$

where the definitions of the terms are retained as in Eq. [1] above.

To the trained eye, Eq. [2] obviously takes the form of an exponential association equation. According to Tsodikov and Record Jr.'s general method of analysis of kinetic equations for multistep processes,[26] for example, declares that the number of exponential terms indicates the number of competing phases or stages—Eq. [2] is therefore a two-phase exponential association. Similarly, Eq. [3] below is a one-phase exponential association equation.

$$D = D_0 + A\left(1 - e^{-a\mathrm{P}}\right) \qquad [3]$$

It is our opinion that Eq. [2] incorporates two dynamic mechanisms of compaction with respect to applied pressure—powder particle rearrangement mechanism, and work hardening mechanisms (the sum of plastic and elastic particle deformation)—not three as per Gerdemann and Jablonski's assignment—we maintain that the bulk density is an initial condition and not a mechanism.

Gerdemann and Jablonski's interpretation of the A, B, D_0, and D_∞ parameters is valid and is consistent with the general method of analysis of exponential association equations. Their interpretation of the 'a and b'

exponent parameters as a reflection of how much pressure is required to bring each mechanism to completion: we however wish to challenge for at least three reasons:

i. The interpretation of the exponent parameters '*a* and *b*', as indicated in Reference 4 is dimensionally incorrect; from Eqs. [1] and [2], '*a* and *b*' must be expressed in terms of MPa^{-1}. Therefore, they cannot be perceived as 'pressures' *per se*.
ii. In addition, exponential association equations analysis schemes generally associate the '*a* and *b*' parameters with rate constants and process half-lives rather than 'parameters required to bring mechanisms to completion'.[26,27]
iii. According to Gerdemann and Jablonski, the typical *a* and *b* parameter values are 21.7×10^3 and 2.99×10^3 MPa, respectively, for ITP CP Ti; 9.51×10^3 and 2.17×10^3 MPa, respectively, for -45 μm TiH_2; and 18.5×10^3 and 1.84×10^3 MPa, respectively, for Ti-6Al-4V, for example.[4] However, these values may not be practically ascertainable (as pressure is required to bring each mechanism to completion) for two likely reasons. First, according to findings summarized in Table II, the onset pressures of the parent-phase to daughter-phase transitions in titanium, titanium alloys, and/or other materials have been consistently observed at pressures as low as 1.8×10^3 MPa at room temperature.[28–32] Such low pressures are easily attainable *via* cold compaction. Second, such structural phase transformations in titanium are generally associated with an inherent volume change collapse in the order of 2 pct to 14 pct.[30,32,33]

It is noted here, for completeness, that exponential association equations have widespread applications mainly in chemical and biological processes, see References 26,27 for further references.

C. *Powder Compaction Curves*

Figure 2 shows the relative density as a function of applied pressure for the four powders under investigation.

There is a notable difference between the compaction behavior of TiH_2-SS316L nanocomposite powders and other studied powder materials. The TiH_2-SS316L nanocomposite powders generally exhibit lower compressibility within the studied pressure range. The difference in the densification behaviors is consistent with a previously noted high yield stress and low plastic deformation propensity in nanostructured powders compared to microstructured powders.[11] The highest densification rate was noticed for the sponge Ti powder throughout the studied pressure range.

All compaction tests show that the density increases with increasing pressure; however, the slope of curves varies remarkably in different pressure ranges. This behavioral characteristic, for all studied powder materials, invariably demonstrates that cold compaction densification is a multi-stage process. In the lower pressure regime ($P < 600$ MPa), the TiH_2 powder material shows marginally higher densification, compared to the Sponge and CP Ti materials, which can tentatively be attributed to the rearrangement of the fracturing hydride powder particles during compaction.

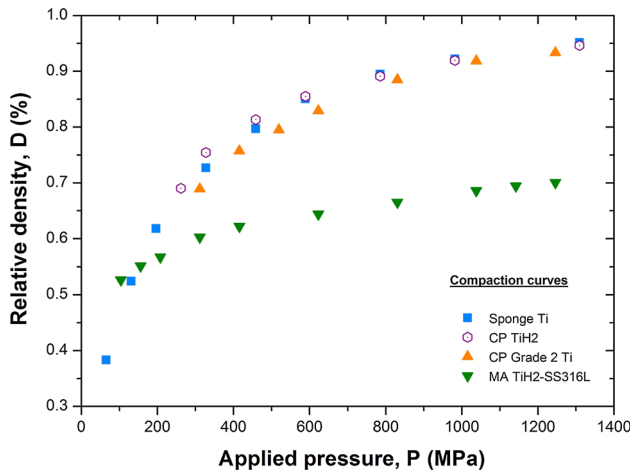

Fig. 2—The compaction characteristics of (*a*) sponge Ti powders, (*b*) TiH_2 powders, (*c*) Grade 2 Ti powder, and (*d*) TiH_2-SS316L nanocomposite powders after 8 h of high energy mechanical milling.

Table II. The Pressure Values at the Onset of the Phase Transitions for Selected Powder Materials (at Room Temperature Conditions)

Material	Phase Transition*	Onset Pressure ($\times 10^3$ MPa)	References
CP Ti	$\alpha \rightarrow \omega$	1.8**	[28–30]
TiH_x	$\delta \rightarrow \varepsilon$ (TiH_2)	2.2	[34–36]
	$\beta + \delta \rightarrow \omega + \eta$ ($TiH_{0.74}$)	7.5†	
TiZr	$\alpha \rightarrow \omega$	~10.0	[33]
Nanostructured Ti	$\alpha \rightarrow \omega$	10.0	[29]
Ti-6Al-4V	$\alpha \rightarrow \omega$	26.2††	[29],[37]
Fe	$\alpha \rightarrow \varepsilon$	11.0	[38]

*α, β, ω, δ, η, and ε represent the HCP alpha-phase, simple BCC beta-phase, hexagonal FCT (distorted BCC) omega-phase, orthorhombic FCC delta-phase, and the monoclinic FCT (distorted BCC) eta-phase.[35]
**Impurities in generally are known to suppress the $\alpha \rightarrow \omega$ structural transfer.[29][39]
†Significantly depended on the amount of H or stoichiometry.[35]
††Implies the onset pressure depends on the pressure transmission medium.[37]

D. *Analysis of Compaction Curves*

Results of the non-linear squares fitting (Eqs. [2] and [3]) of the experimental compaction response data, for the powders under investigation, are shown in Figure 3.

With the exception of CP Grade 2 Ti powder, nonlinear least squares fitting of a one-phase exponential association equation to the experimental data gives a marginally inferior fit, as shown in Figure 3. However, predicting the compaction density *vs* pressures profiles alone without parameters that *'relate in some way to the basic physical and mechanical properties of the material being compacted'* falls short on Denny's criterion[12] of an ideal multi-stage compaction equation. Thus, the underlying mechanisms driving the compaction process seemingly cannot be described completely in terms of a one-phase exponential association equation.

True to published claims[4]; the regression analysis confirms good applicability of the Gerdemann–Jablonski compaction model. It gives a good fit ($R^2 > 99.50$ pct) to experimental data for all powder materials regardless of powder characteristics over the entire pressure range of the experiment.

In this study, the fit parameters in Eq. [2], for all the titanium powder materials, were determined simultaneously by means of non-linear least squares analysis of the experimental data. Curve fitting was done with the software OriginPro (OriginLab Corporation). The results are summarized in Table II below.

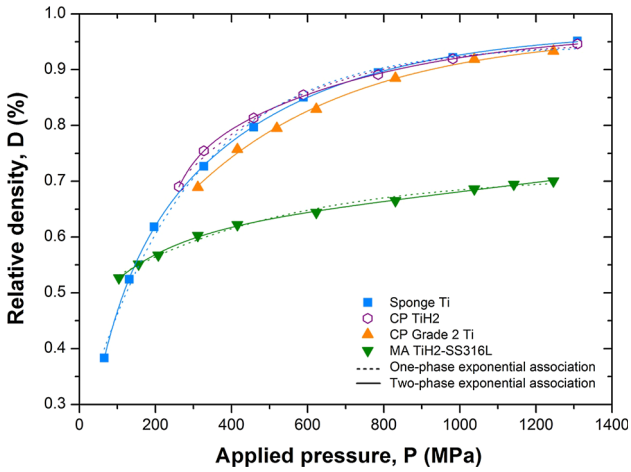

Fig. 3—The relative density *vs* applied pressure data (shown also in Fig. 2) fitted with the Gerdemann–Jablonski model (Eq. [2]).

The model deduced initial densities of the sponge Ti and mechanically alloyed Ti nanostructured powder material are in close agreement to the experimentally determined values. The model deduced initial densities of the TiH_2 and Grade 2 Ti powder materials are however not in good agreement. The model determined maximum achievable density, D_∞, are in very close agreement to the values determined from the experimental compaction curves.

The fitting is also extrapolated toward the low pressure range to illustrate the possible interpretation of the *'a* and *b'* model parameters—*i.e.* the process half-lives of powder particle rearrangement ($\ln 2/a$) and the particle work hardening mechanism ($\ln 2/b$). A kinetic analysis of the densification mechanisms also reveals process rate constants as well as the process half-life values. The analysis yields process half-life values of 54.65 and 277.11 MPa for the rearrangement and work hardening densification mechanisms, respectively, for Ti sponge powder. Using the fit parameters tabulated in Table III and Eq. [2], it is possible to separate the contributions and kinetics (pressure variations) of the powder particle rearrangement and the particle work hardening mechanisms of densification. The sponge Ti material was used here as an example, as shown in Figure 4. The fractional contribution of the densification mechanisms and initial density to D_∞ are also illustrated therein.

Table IV shows the relative fractional contributions of the particle rearrangement and work hardening mechanisms of densification, with respect to the maximum achievable density. Consistent with Gerdemann–Jablonski's observations, powder materials with mixed morphologies (sponge Ti and MA TiH_2-SS316L) had the relatively lowest contribution from the rearrangement term and the Grade 2 Ti powders with a spherical morphology have a more significant contribution from the rearrangement mechanism.

IV. SUMMARY AND CONCLUSIONS

The validity and applicability of the Gerdemann and Jablonski's proposed compaction were experimentally

Table III. Fit Parameters to Eqs. [2] and [3] for the Powder Materials Under Investigation

	D_0 (pct)	A	B	D_∞	$\ln 2/a$ (MPa)	$\ln 2/b$ (MPa)	Adj. R^2 (pct)
Equation [3]							
Ti sponge	0.257307	0.686841		0.944148	85.16		99.50
TiH_2	0.40014	0.55156		0.9517	101.06		99.12
CP grade 2 Ti	0.399078	0.567005		0.966083	129.15		99.46
MA TiH_2-SS316L	0.488258	0.224604		0.712861	145.03		99.13
Equation [2]							
Ti sponge	0.1329	0.2912	0.53844	0.9626	54.65	277.11	99.98
TiH_2	0.1291	0.4270	0.4210	0.9771	70.17	333.54	99.94
CP grade 2 Ti	0.1077	0.5514	0.3660	1.0240	112.37	605.89	99.51
MA TiH_2-SS316L	0.4545	0.1171	0.1623	0.7339	122.02	602.35	99.81

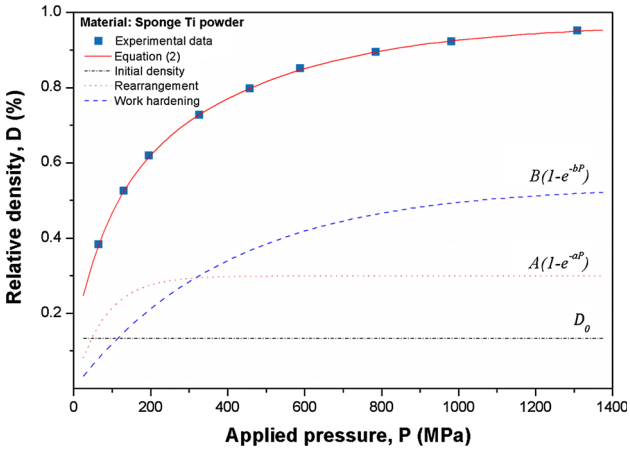

Fig. 4—The variations of the powder rearrangement and work hardening mechanisms with pressure in the sponge Ti powder material.

Table IV. Relative Fractional Contributions of the Particle Rearrangement and Work Hardening Mechanisms to the Maximum Achievable Densities

	Particle Rearrangement (Pct)	Work Hardening (Pct)
Ti sponge + 180 μm	35.10	64.90
TiH_2	50.36	49.64
Gd.2Ti	60.11	39.89
MA TiH_2-SS316L	41.91	58.09

evaluated. Results from the enquiry conducted are summarized as following:

i. The Gerdemann–Jablonski compaction equation takes the form of a two-phase exponential association equation. It incorporates two dynamic mechanisms of compaction—particle rearrangement and work hardening mechanisms (the sum of plastic and elastic particle deformation)—not three mechanisms as per Gerdemann and Jablonski's interpretation—the bulk density is an initial condition and not a mechanism.
ii. Analysis for all powder materials studied over the entire pressure range tested confirms that densification cannot be described completely in terms of a single densification mechanism. The Gerdemann–Jablonski compaction equation shows better applicability with higher correlation coefficients compared to the one-phase exponential association equation. However, when a single mechanism dominates densification, the one-phase exponential association equation also exhibits high correlation coefficient.
iii. The application of Gerdemann–Jablonski compaction equation permits the deconvolution of relative contributions and kinetics (variations with respect to pressure) of the densification mechanisms.
iv. Our analysis confirms the validity of Gerdemann and Jablonski's interpretation of A, B, D_0, and D_∞ model parameters. However, Gerdemann and Jablonski's interpretation of the 'a and b' model exponent parameters is challenged; an alternative interpretation is proposed based on the general analysis of two-phase exponential association equation—*i.e.* $(\ln 2/a)$ and $(\ln 2/b)$ quantify the process half-lives of the powder particle rearrangement and the particle work hardening mechanisms, respectively.

ACKNOWLEDGMENTS

We are grateful to Thembinkosi Shabalala—for his contribution during the preparation of the mechanically blended powder—and to Jeff Benson—for his comments on the early versions of this paper. The contributions of Chris Machio and Silethelwe Chikosha especially are gratefully recognized. This research has been financially supported by the Department of Science and Technology through the Titanium Centre of Competence research program and the Council for Scientific and Industrial Research.

REFERENCES

1. P. Paronen and J. Llkka: in *Pharmaceutical Powder Compaction Technology*, G. Alderborn and C. Nystrom, eds. CRC Press, Florida, 1995, pp. 55–75.
2. G. Bockstiegel: *Proc. Int. Powder Met. Conf.*, 1966, vol. 1, pp. 155–87.
3. P.Y. Huang: *Powder Metallurgy Principle*, Metallurgical Industry Press, Beijing, 1982, pp. 373–74.
4. S.J. Gerdemann and P.D. Jablonski: *Metall. Mater. Trans. A*, 2011, vol. 42A, pp. 1325–33.
5. F.H. Froes, S.J. Mashl, J.C. Hebeisen, V.S. Moxson, and V.A. Duz: *JOM*, 2004, vol. 56 (11), pp. 46–48.
6. J.M. Sonnergaard: *Eur. J. Pharm. Sci.*, 2001, vol. 14 (2), pp. 149–57.
7. P. Adapa, L. Tabil, and G. Schoenau: *Biosyst. Eng.*, 2009, vol. 104 (3), pp. 335–44.
8. S. Mallick: *J. Sci. Ind. Res.*, 2014, vol. 73 (January), pp. 51–56.
9. K. Katsuyoshi and W. Ryuzo: *Trans. JWRI*, 2006, vol. 35 (2), pp. 47–51.
10. A.R. Cooper and L.E. Eaton: *J. Am. Ceram. Soc.*, 1962, vol. 45 (3), pp. 97–101.
11. D. Jeyasimman, K. Sivaprasad, S. Sivasankaran, and R. Narayanasamy: *Powder Technol.*, 2014, vol. 258, pp. 189–97.
12. P.J. Denny: *Powder Technol.*, 2002, vol. 127 (2), pp. 162–72.
13. M. Qian: *Int. J. Powder Metall.*, 2010, vol. 46 (5), pp. 29–44.
14. R. Frykholm and H. Vidarsson: "Ti Alloys in PM Applications", in *World Congress PM2014 in Orlando*, 2014.
15. W. Chen, Y. Yamamoto, W.H. Peter, M.B. Clark, S.D. Nunn, J.O. Kiggans, T.R. Muth, C.A. Blue, J.C. Williams, and K. Akhtar: *J. Alloys Compd.*, 2012, vol. 541, pp. 440–47.
16. A. Jimoh, I. Sigalas, and M. Hermann: *J. Sci. Technol. Math. Educ.*, 2011, vol. 7 (2), pp. 42–52.
17. P.G. Esteban, Y. Thomas, E. Baril, E.M. Ruiz-Navas, and E. Gordo: *Met. Mater. Int.*, 2011, vol. 17 (1), pp. 45–55.
18. S.-T. Hong, Y. Hovanski, C.A. Lavender, and K.S. Weil: *J. Mater. Eng. Perform.*, 2008, vol. 17 (3), pp. 382–86.
19. S. Chikosha, T.C. Shabalala, and H.K. Chikwanda: *Powder Technol.*, 2014, vol. 264, pp. 310–19.

20. E.M. Borisovskaya, V.A. Nazarenko, Y.N. Podrezov, O.S. Koryak, Y.I. Evich, and V.F. Gorban: *Powder Metall. Met. Ceram.*, 2008, vol. 47 (7–8), pp. 406–13.
21. J.B. Lim, C.J. Bettles, B.C. Muddle, and N.K. Park: *Mater. Sci. Forum*, 2010, vols. 654–656, pp. 811–14.
22. K.K. Sobiyi: *Machining Of Powder Metal Titanium*, University of Stellenbosch, 2011.
23. J. Lou and B. Gabbitas: in *International Titanium Powder Processing, Consolidation and Metallurgy Conference*, 2013.
24. ASTM D7481—09 Standard Test Methods for Determining Loose and Tapped Bulk Densities of Powders using a Graduated Cylinder, *Book of Standards Volume: 04.09*. ASTM International, West Conshohocken, PA, 2009.
25. Test Methods Used During Development or Manufacture: Bulk Density and Tapped Density of Powders, *Supplementary Information in The International Pharmacopoeia, 4th Edition*. WHO, Geneva, Switzerland, 2014.
26. O.V. Tsodikov and M.T. Record: *Biophys. J.*, 1999, vol. 76 (3), pp. 1320–29.
27. H. Motulsky and A. Christopoulos: *Fitting Models to Biological Data Using Linear and Nonlinear Regression: A Practical Guide to Curve Fitting*, Oxford University Press, 2004, pp. 317–19.
28. Z.-G. Mei, S.-L. Shang, Y. Wang, and Z.-K. Liu: *Phys. Rev. B*, 2009, vol. 80 (10), p. 104116.
29. N. Velisavljevic, S. MacLeod, and H. Cynn: in *Titanium Alloys—Towards Achieving Enhanced Properties for Diversified Applications*, A.K.M.N. Amin, ed. InTech, 2012, pp. 67–86.
30. D. Errandonea, Y. Meng, M. Somayazulu, and D. Häusermann: *Phys. B Condens. Matt.*, 2005, vol. 355 (1–4), pp. 116–25.
31. D. Trinkle, R. Hennig, S. Srinivasan, D. Hatch, M. Jones, H. Stokes, R. Albers, and J. Wilkins: *Phys. Rev. Lett.*, 2003, vol. 91 (2), p. 025701.
32. J. Zhang, Y. Zhao, R.S. Hixson, G.T. Gray, L. Wang, W. Utsumi, S. Hiroyuki, and H. Takanori: *J. Phys. Chem. Solids*, 2008, vol. 69 (10), pp. 2559–63.
33. V. Dmitriev, L. Dubrovinsky, T. Bihan, A. Kuznetsov, H.-P. Weber, and E. Poniatovsky: *Phys. Rev. B*, 2006, vol. 73 (9), p. 094114.
34. N. Endo, H. Saitoh, A. Machida, Y. Katayama, and K. Aoki: *J. Alloys Compd.*, 2013, vol. 546, pp. 270–74.
35. I.O. Bashkin, V.K. Fedotov, H.-J. Hesse, A. Schiwek, W.B. Holzapfel, and E.G. Ponyatovsky: *J. Phys.*, 2002, vol. 14 (5), pp. 955–66.
36. P.E. Kalita, A.L. Cornelius, K.E. Lipinska-Kalita, C.L. Gobin, and H. Peter Liermann: *J. Phys. Chem. Solids*, 2008, vol. 69 (9), pp. 2240–44.
37. S.G. MacLeod, B.E. Tegner, H. Cynn, W.J. Evans, J.E. Proctor, M.I. McMahon, and G.J. Ackland: *Phys. Rev. B*, 2012, vol. 85 (22), p. 224202.
38. E. Huang, W. A. Bassett, and P. Tao: in *High-Pressure Research in Mineral Physics: A Volume in Honor of Syun-iti Akimoto*, vol. 39, M.H. Manghnani and Y. Syono, eds. Washington, D. C.: American Geophysical Union, 1987, pp. 165–72.
39. R.G. Hennig, D.R. Trinkle, J. Bouchet, S.G. Srinivasan, R.C. Albers, and J.W. Wilkins: *Nat. Mater.*, 2005, vol. 4 (2), pp. 129–33.